arXiv:physics/0511123v3 [physics.optics] 6 Mar 2006

Pump-probe nonlinear magneto-optical rotation with frequency modulated light

S. Pustelny,[1] D. F. Jackson Kimball,[2] S. M. Rochester,[3] V. V. Yashchuk,[4] W. Gawlik,[1] and D. Budker[3,5]

[1]*Instytut Fizyki im. M. Smoluchowskiego, Uniwersytet Jagielloński, Reymonta 4, 30-059 Kraków, Poland*
[2]*Department of Physics, California State University – East Bay, 25800 Carlos Bee Blvd., Hayward, CA 94542, USA*
[3]*Department of Physics, University of California at Berkeley, Berkeley, CA 94720-7300, USA*
[4]*Advanced Light Source Division, Lawrence Berkeley National Laboratory, Berkeley CA 94720, USA*
[5]*Nuclear Science Division, Lawrence Berkeley National Laboratory, Berkeley CA 94720, USA*

(Dated: February 2, 2008)

Specific types of atomic coherences between Zeeman sublevels can be generated and detected using a method based on nonlinear magneto-optical rotation with frequency modulated light. Linearly polarized, frequency modulated light is employed to selectively generate ground-state coherences between Zeeman sublevels for which $\Delta m = 2$ and $\Delta m = 4$ in ^{85}Rb and ^{87}Rb atoms, and additionally $\Delta m = 6$ in ^{85}Rb. The atomic coherences are detected with a separate, unmodulated probe light beam. Separation of the pump and probe beams enables independent investigation of the processes of creation and detection of the atomic coherences. With the present technique the transfer of the Zeeman coherences, including high-order coherences, from excited to ground state by spontaneous emission has been observed.

PACS numbers: 32.80.Bx,33.55.Be,42.65.An,42.62.Fi

I. INTRODUCTION

The use of light to create and detect coherences between atomic states, and the evolution of those coherences when the atomic states are nondegenerate, is a powerful method for precision spectroscopy, extensively employed for measurements of external fields, tests of fundamental symmetries (see, for example, reviews [1] and [2]), and and frequency standards [3]. In this work, we report an experimental technique to selectively create and detect atomic coherences between Zeeman sublevels ($\Delta m = 2, 4, 6$) in the ground states of alkali atoms. We employ two independent laser beams, one for creation of the ground state coherences and a second for detection of the coherences, allowing detailed experimental studies of the optical pumping and probing processes. Selective creation and detection of the $\Delta m = 6$ coherence was achieved for the first time, and transfer of high-order Zeeman coherences from the excited state to the ground state via spontaneous emission was observed.

Resonant nonlinear magneto-optical rotation (NMOR) has been studied for over 30 years (see the review [2] and references therein). The essence of the effect is light-intensity-dependent rotation of the polarization plane of a beam of light propagating through a medium placed in a magnetic field. Most often the effect is studied in the Faraday geometry, in which the magnetic field is applied along the direction of light propagation. The NMOR signals can either be observed as a function of magnetic field with the laser frequency fixed (magnetic-field domain), or as a function of the laser frequency with the magnetic field fixed (spectral domain). There are several effects that contribute to NMOR signals. These contributions can be distinguished in the magnetic-field domain as they typically give rise to optical rotation that peaks at different values of the magnetic field (leading to a group of nested dispersive features). In general, the width of the narrowest feature is determined by the effective rate of relaxation of atomic ground-state coherences. In evacuated (buffer-gas-free) cells with anti-relaxation coating, ground-state coherences can be preserved for 500 ms or longer, leading to NMOR signals with sub-Hertz widths [4, 5].

The dispersive features in the magnetic field dependence observed in a NMOR experiment with unmodulated light are centered at zero magnetic field. This restricts magnetic field measurements using NMOR to values of the magnetic field for which Larmor frequencies are smaller than the ground-state relaxation rate. However, combining the NMOR effect with the technique of synchronous optical pumping [6] allows one to obtain similarly narrow NMOR features centered at non-zero magnetic fields, including the Earth-field range important for many applications (see Ref. [1] and references therein). Such resonances generally appear when a harmonic of the modulation frequency is a particular multiple of the Larmor frequency.

The synchronous pumping of atoms in NMOR enables a selective creation of high-rank atomic polarization moments (PMs) associated with high-order Zeeman coherences. The PMs are described by the density matrix elements in the irreducible tensorial basis [7, 8] (see Section II below). Such moments and associated atomic coherences have drawn attention [9, 10, 11] because they may enhance nonlinear optical effects important in such applications as quantum gates [12], electromagnetically induced transparency [13, 14], and magnetometry [7, 15, 16, 17].

In this paper we investigate selective creation and detection of atomic ground-state PMs of rank $\kappa = 2$, $\kappa = 4$, and $\kappa = 6$, corresponding to coherences between Zeeman sublevels with $\Delta m = 2, 4$ and 6, respectively, via

interaction with linearly polarized, frequency modulated light (FM NMOR) [30]. Two independent light beams interacting with atoms via different excited states enable detailed analysis of the processes of creation and detection of atomic multipoles in the ground state. Specifically, we have measured the signal dependences on pump and probe-beam tuning and intensity. We have observed that the signals depend differently on pump- and probe-light parameters, which is important for optimization of magnetometry schemes based on FM NMOR. Separated pump and probe beams may also be necessary for a more efficient method of production of high-rank multipoles, wherein pumping and probing are done at different harmonics of the Larmor frequency [18].

The article is organized as follows. In Section II the FM NMOR method is described in detail. The symmetries of the atomic PMs are shown and mechanism by which a specific PM is generated is explained. In Section III the experimental setup for pump-probe FM NMOR is discussed. Section IV presents the experimental results and their analysis. In particular, the dependences of the FM NMOR-resonance amplitudes and widths on pump and probe intensities and frequencies are presented and discussed. Also the results are shown demonstrating coherences transfer via spontaneous emission. Finally, conclusions are summarized in Section V.

II. GENERATION AND DETECTION OF ATOMIC COHERENCES AND ATOMIC POLARIZATION MOMENTS

The density matrix written in the M, M' representation for a state with total angular momentum F can be decomposed into PMs of rank $\kappa = 0, 1, \ldots, 2F$ (also known as multipoles of order $k = 2^\kappa$) with components $q = -\kappa, -\kappa+1, \ldots, \kappa$:

$$\rho_q^{(\kappa)} = \sum_{M,M'=-F}^{F} (-1)^{F-M'} \langle F, M, F, -M' | \kappa, q \rangle \rho_{MM'}, \tag{1}$$

where $\langle \ldots | \ldots \rangle$ are the Clebsch-Gordan coefficients. The PM components transform as

$$\rho_q^{(\kappa)} \to e^{-iq\phi} \rho_q^{(\kappa)} \tag{2}$$

when the PM rotates by an angle ϕ about the quantization axis. Interaction of light with an unpolarized sample (having only the $\rho_0^{(0)}$ moment, which is proportional to the population distribution) causes redistribution of atomic population and creation of coherences among the Zeeman sublevels, generating higher-order moments (components $\rho_q^{(\kappa)}$ are related to coherences with $\Delta M = |q|$). With a single photon-atom interaction, a PM of rank $\kappa \leq 2$ with components $|q| \leq 2$ can be generated. Creation of PMs with higher components $|q| > 2$ requires multi-photon interactions between light and matter. Once the PMs are created in the medium, the same number of photon interactions as needed for their creation are required for the PMs to affect the properties of the transmitted light. This can be understood by recalling that a photon is a spin-one particle, so it is described by a tensor operator of rank $\kappa \geq 2$.

Generally if the light intensity is sufficiently high to produce the high-rank PM, it will also produce all the lower-rank moments with greater or equal efficiency. Therefore it has been difficult to distinguish effects related to high-rank PMs from those associated with lower-rank PMs.

One method for generating and detecting specific PMs in a medium, as reported in Ref. [7], is FM NMOR, in which pump-light is modulated periodically bringing the light frequency on and off resonance with the atoms, and effectively creating optical pumping pulses. With linearly polarized light, atomic PMs of even rank [31] are created, which precess around the magnetic field, i.e., undergo continuous rotation according to Eq. (2), with $\phi = \Omega_L t$, where Ω_L is the Larmor frequency. If the modulation frequency Ω_{mod} and the Larmor frequency are not commensurate, the transverse polarization (components with $q \neq 0$) created in successive pumping cycles will add with different phases, and will wash out after multiple pumping pulses. However, if $\Omega_{mod} = n\Omega_L$, where n is an even number, the transverse PMs with less than n-fold symmetry ($0 < |q| < n$) will average out, but those with $|q| \geq n$ will be reinforced. This can be visualized using a method described, for example, in Ref. [19]. On a particular cycle of the optical-pumping modulation (thought of as a short pulse for the purposes of this illustration), PMs of all even ranks up to $\kappa = 2F$ are created in the ground state, with the lowest-order moment (quadrupole) dominating at low power. The quadrupole moment [Fig. 1(a)] has an axis along the light polarization (y-axis) and a corresponding symmetry of order 2 about the z-axis. If modulation occurs at $4\Omega_L$, the PM will have rotated one-fourth of a cycle (90°) by the next pump pulse [Fig. 1(b)]. The average of the rotated PM and the newly pumped quadrupole moment is symmetric with respect to the z-axis, i.e., the transverse polarization has averaged out [Fig. 1(c)]. (Any remaining transverse polarization would have fourth-fold symmetry with respect to the z-axis, which cannot be supported by the quadrupole moment, with $|q| \leq \kappa = 2$.) The longitudinal quadrupole component $\rho_0^{(2)}$, symmetric with respect to the z-axis, does remain, but it is not affected by the magnetic field nor does it cause optical rotation. Because the transverse quadrupole moment has been destroyed, the transverse hexadecapole moment is now the lowest-order contributor to the FM NMOR signal (for $F = 2$ it is the only transverse moment remaining). For this moment, the pumped PM [Fig. 1(d)] averaged with the PM rotated by 90° [Fig. 1(e)] does leave transverse polarization remaining [Fig. 1(f)], because the hexadecapole moment can support fourth-fold symmetries. (The second-fold symmetry, corresponding to $|q| = \Delta M = 2$ is destroyed, but the $\rho_{\pm 4}^{(4)}$ components remain.) Thus the low-order

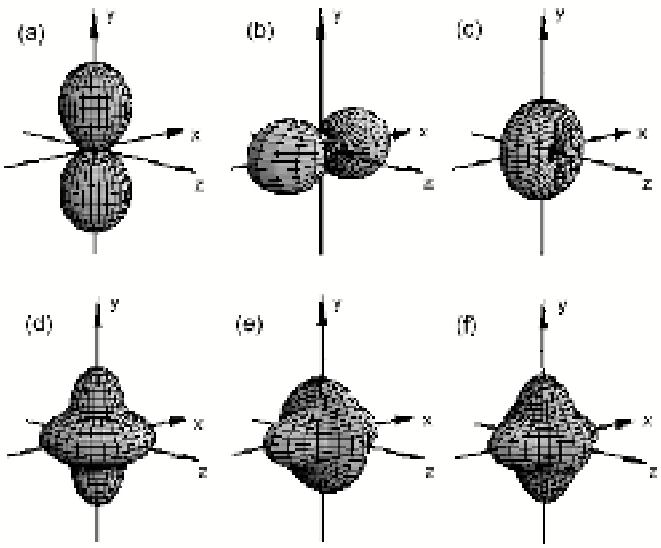

FIG. 1: Visualization of the averaging of the PMs. The surface distance from the origin in a given direction is equal to the probability of finding the highest projection of the angular momentum ($M = F$) in that direction. The quadrupole and hexadecapole moments created in the medium due to interaction with light polarized along y-axis are shown in (a) and (d). After creation the atomic polarization rotates around the magnetic field applied along z-axis. If the pumping is modulated at four times the Larmor frequency newly created multipoles (a) and (d) are rotated by 90° with respect to the previously created quadrupole (b) and hexadecapole (e) moments. The resultant polarization of the medium after many pumping cycles related to quadrupole and hexadecapole is shown in (c) and (f). Since the averaged quadrupole is symmetric with respect to rotation around z-axis the time-dependent changes of the optical anisotropy of the medium affecting light propagating along z-axis are related only to the hexadecapole moment. The plots are drawn for an $F = 2$ state.

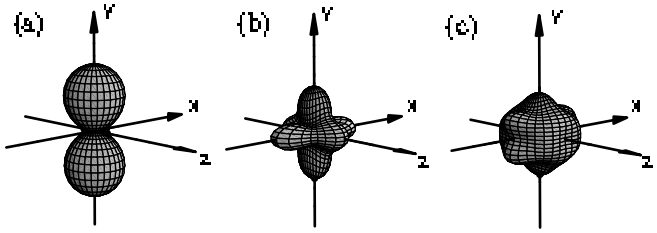

FIG. 2: The averaged PMs: two-fold symmetric quadrupole (a), four-fold symmetric hexadecapole (b), and six-fold symmetric hexacontatetrapole (c). Each of the averaged PMs is associated with the Zeeman coherences in the ground state: averaged quadrupole with $\Delta m = 2$, averaged hexadecapole with $\Delta m = 4$, and averaged hexacontatetrapole with $\Delta m = 6$. The plots are drawn for an F=3 state.

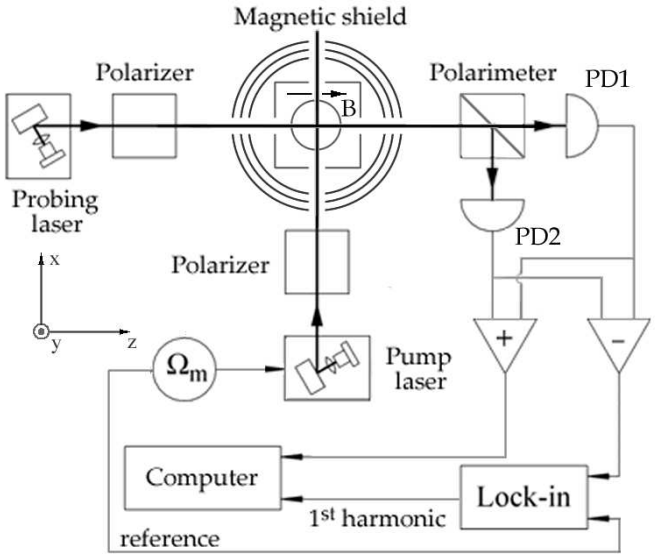

FIG. 3: Experimental setup. PD1 and PD2 are photodiodes.

transverse PMs are eliminated, leaving, in general, only PMs with $|q|$ greater than or equal to n.

The precession of the transverse PMs in the magnetic field results in time-varying optical rotation in the probe light beam. In our experimental arrangement, the signal is proportional to the amplitude of the optical rotation at various harmonics of the modulation frequency. The optical pumping resonance at $\Omega_{mod} = n\Omega_L$, producing polarization moments with $|q| \geq n$, leads to resonance features in the signal [7, 20, 21]. Because the PM components have $|q|$-fold symmetry, the signal that they create in the probe beam is at the frequency $|q|\Omega_L$ (Fig. 2). Thus if observations are made at the first harmonic of the modulation frequency, only the components with $|q| = n$ will contribute to the signal. For example, ^{87}Rb has a resonance related to the $|q| = 2$ components of the quadrupole and hexadecapole moments ($\rho^{(2)}_{\pm 2}$ and $\rho^{(4)}_{\pm 2}$) appearing at $\Omega_{mod} = 2\Omega_L$, and a resonance related to the $|q| = 4$ components of the hexadecapole moment ($\rho^{(4)}_{\pm 4}$) at $\Omega_{mod} = 4\Omega_L$. In ^{85}Rb an extra resonance appears at $\Omega_{mod} = 6\Omega_L$, which it is related to the $|q| = 6$ components of the hexacontatetrapole ($\kappa = 6$) moment ($\rho^{(6)}_{\pm 6}$).

The appearance of these narrow resonances at high magnetic fields allows NMOR-based magnetometry with no trade-off between dynamic range and sensitivity. In addition, the separated pump and probe technique used in this work enables independent investigation of creation and detection of the PMs.

III. EXPERIMENTAL SETUP

The experiment is an extension of the previous experiments [7, 20, 21] in which FM NMOR was studied with a single light beam. The scheme of the present experiment is shown in Fig. 3. The atomic vapor cell is placed in a four-layer magnetic shield. The shield provides passive attenuation of dc fields to a level of 1 part in 10^6 [22]. Magnetic coils mounted inside the shield are used

for compensation of residual magnetic fields and their first-order gradients. They are also used to produce a bias magnetic field along the z-axis.

The separated pump and probe beams, each 2 mm in diameter, interact with an isotopically enriched sample of ^{85}Rb or ^{87}Rb atoms contained in a buffer-gas-free, paraffin-coated, 10 cm diameter spherical cells. The coating of the cell walls allows the lifetime of atomic PMs in the ground state in the absence of light to be up to 500 ms. The external-cavity diode laser (pump laser) produces light at 795 nm for the rubidium D1 line ($^2S_{1/2} \rightarrow ^2P_{1/2}$). In most cases, for ^{87}Rb measurements, the central frequency of the laser is tuned to the low-frequency wing of the $F = 2 \rightarrow F' = 1$ transition (see ^{87}Rb spectrum of the D1 line in Fig. 8(c)), while for ^{85}Rb measurements it is tuned to the center of the $F = 3 \rightarrow F'$ transition group (see ^{85}Rb spectrum of the D1 line in Fig. 16(b)). In both cases the laser central frequency is stabilized with a dichroic atomic vapor laser lock [23, 24] modified for operation with frequency modulated light. Synchronous pumping of atoms is achieved with frequency modulated pump-light. The modulation frequency ranged from 70 Hz up to 1 kHz with 300 MHz (peak to peak) modulation depth. The unmodulated probe laser generates light at 780 nm for the rubidium D2 line ($^2S_{1/2} \rightarrow ^2P_{3/2}$). The frequency of the probe laser is stabilized and tuned, in most cases for the ^{87}Rb measurements, to the center of the $F = 2 \rightarrow F''$ transition group (see ^{87}Rb spectrum of the D2 line in Fig. 11(c)) and, for ^{85}Rb measurements, to the center of the $F = 3 \rightarrow F''$ transition group. The use of two light beams interacting with atoms via different excited states (D1 and D2 transitions) ensures, in addition to the small crossing area of the pump and probe beams inside a shield, that the optical rotation is only due to the polarization in the ground state [32].

The light beams are perpendicular; the pump beam propagates along x-axis and the probe beam propagates along z-axis, parallel to the magnetic field. Both beams are linearly polarized along y-axis before entering a cell.

Upon passing through the cell the polarization of the probe beam is modulated due to the precessing anisotropy of the medium. The polarization is analyzed using a balanced polarimeter. In the polarimeter two photodiodes detect transmission through a polarizing beam-splitter at 45° to the incident light beam polarization in the x-y plane. The amplitude of the photodiode difference signal is detected with a lock-in amplifier at the first harmonic of Ω_{mod}. The FM NMOR resonances were recorded by scanning Ω_{mod}.

IV. RESULTS AND ANALYSIS

In this section the experimental results and their analysis are presented. The typical two-beam FM NMOR signal is discussed and compared with the single-beam FM NMOR signal. We then discuss the dependences

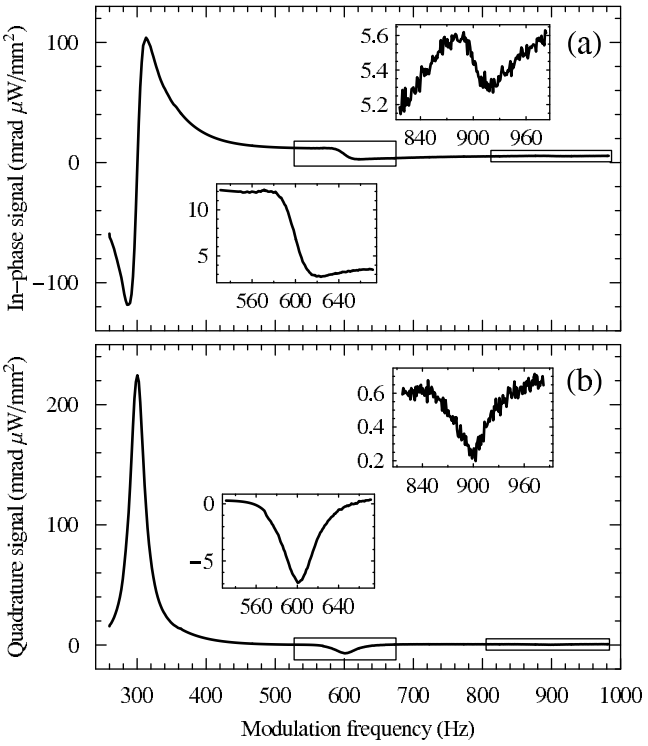

FIG. 4: The two-beam FM NMOR in-phase (a) and quadrature (b) signals in the modulation-frequency domain with fixed magnetic field ($\Omega_L \approx 2\pi \times 150$ Hz). Signals at ≈300 Hz, ≈600 Hz, and ≈900Hz are related to the two-fold symmetric multipoles (mostly quadrupole), four-fold symmetric multipoles (mostly hexadecapole) and six-fold symetric (hexacontatetrapole) moment, respectively. The insets show magnification of the hexadecapole and hexacontaterapole resonances. The signals were recorded in ^{85}Rb with $I_{pump} = 17$ μW/mm^2 and $I_{probe} = 20$ μW/mm^2. Pump laser was tuned to the center of the $F = 3 \rightarrow F'$ transition group and probe laser to the high-frequency wing of the $F = 3 \rightarrow F''$ transition group. The units of the signal correspond to the rotation of the polarization plane of the probe beam multiplied by the probe-beam intensity. In order to calculate the angle of the rotation the recorded signal should be divided by the probe-light intensity.

of the two-beam signals on the pump- and probe-beam parameters, to understand the detailed mechanisms of creation and detection of atomic multipoles.

A representative recording of the two-beam FM NMOR signal in the modulation-frequency domain measured in ^{85}Rb is presented in Fig. 4. Three resonances were observed centered at twice (≈300 Hz), four times (≈600 Hz), and six times (≈900 Hz) the Larmor frequency ($\Omega_L \approx 2\pi \times 150$ Hz). As discussed in Section II, these resonances are related to the two-fold symmetric multipoles (mostly quadrupole $\rho^{(2)}_{\pm 2}$ but also with some hexadecapole $\rho^{(4)}_{\pm 2}$ and hexacontatetrapole $\rho^{(6)}_{\pm 2}$ admixture), four-fold symmetric hexadecapole and hexacontatetrapole moments, $\rho^{(4)}_{\pm 4}$ and $\rho^{(6)}_{\pm 4}$, respectively and pure six-fold symmetric hexacontatetrapole $\rho^{(6)}_{\pm 6}$. Accord-

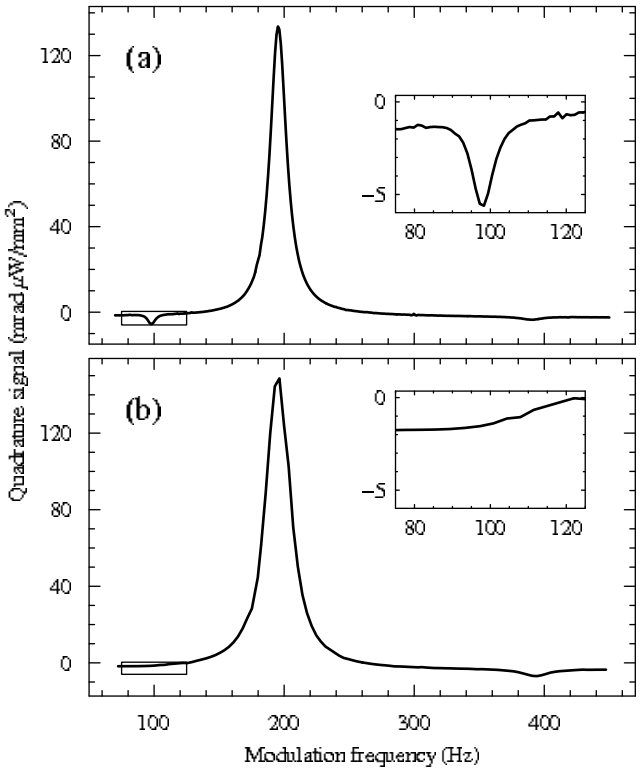

FIG. 5: Single-beam (a) and two-beam (b) FM NMOR signals measured in ^{87}Rb. The upper inset shows a magnification of the resonance ($\Omega_{mod} \approx 2\pi \times 97.5$ Hz) appearing due to the modulation of the probe light in single-beam FM NMOR. The lower inset shows the absence of that signal in the two-beam arrangement. The pump-beam central frequency and probe-beam frequency were tuned to the low-frequency wing of the $F = 2 \rightarrow F' = 1$ transition of the D1 line and the center of the $F = 2 \rightarrow F''$ transition group of the D2 line, respectively, in the two-beam experiment. In the single-beam FM NMOR experiment light was tuned to the low-frequency wing of the D1 line. The intensities of the pump and probe in the two-beam experiment were the same ($I_{pump} = I_{probe} = 20$ μW/mm^2), half of the intensity of the incident light in the single-beam experiment ($I = 40$ μW/mm^2).

ing to the authors' best knowledge, signal observed at six-times the Larmor frequency (hexacontatetrapole resonance) is the first observation of an effect related solely to the $\Delta m = 6$ coherences. A detailed analysis of selective creation and detection of this type of coherences is given in Section IV C.

A comparison of single-beam and two-beam resonances is given in Fig. 5. In the single-beam FM NMOR experiment [7, 20, 21] the medium is pumped and probed with the same, frequency-modulated laser beam. Because in this case the probe light is modulated, additional resonances occur that do not appear in the two-beam case (see insets in Fig. 4). At $\Omega_{mod} = 2\Omega_L$ the quarupole is efficiently pumped (this is a resonance which is part of the an $\Omega_{mod} = 2\Omega_L$ family of resonances for quadrupole), but there is no signal observed at the first harmonic for unmodulated probe light as the polarization is modulated by the medium at $2\Omega_L$, i.e., at the second harmonic of Ω_{mod}. However, when the probe is modulated, this leads to the first-harmonic signal as observed in the single-beam experiment (Fig. 5(a)). Thus, unlike the two-beam experiment with unmodulated probe, a resonance appears at $\Omega_{mod} = \Omega_L$ (compare the resonance at $\Omega_{mod} \approx 2\pi \times 97.5$ Hz in Fig. 5(a) with the absence of one in Fig. 5(b)).

Below we present the dependence of FM NMOR resonances' amplitudes and widths as a function of pump- and probe-light parameters. The amplitudes and widths of the FM NMOR resonances were determined by fitting the dispersive-like Lorentzians ($Ax/(x^2 + \delta\Omega_{mod}^2)$ to the in-phase component and absorptive-like Lorentzians ($A/(x^2 + \delta\Omega_{mod}^2)$ to the quadrature component of the recorded signals. Within our experimental conditions the amplitudes and widths determined in both components of the signals are the same.

The discussion in the two next subsections refers to data taken with ^{87}Rb. The ^{87}Rb data obtained as a function of pump- and probe-beam parameter are considered separately in order to facilitates the comparison between creation and detection of the atomic PMs. In Section IV C the ^{85}Rb data is discussed.

A. Creation of atomic PMs

The amplitudes of the quadrupole and hexadecapole FM NMOR resonances are plotted vs. pump-light intensity in Fig. 6. The probe beam was attenuated to 1.6 μW/mm^2 to simplify the interpretation of the results. However, the drawback of choosing such probe-light intensity is that at low pump-beam intensities only the quadrupole signal could be observed. The hexadecapole signal was measured at pump intensities above 5 μW/mm^2.

At low intensities, the quadrupole amplitude scales linearly with pump-light intensity. This is because only a one-photon interaction is needed for the creation of the quadrupole moment. However, as the pump-beam intensity increases the curve tends to grow slower than linear with I_{pump} due to higher-order effects. We will refer to these generally as saturation effects, although they may include more complex processes such as alignment-to-orientation conversion and related phenomena (see, for example, Ref. [25]). Although the lack of low pump-intensity data for the hexadecapole moment preclude reliable determination of the intensity dependence in the low-intensity limit, the data are not inconsistent with the expected quadratic behavior.

As can be seen in Fig. 6 the amplitude of the quadrupole and hexadecapole signals differ by at least two orders of magnitude. As pointed out by M. Auzinsh, it may be possible to generate the hexadecapole moment more efficiently by pumping at $2\Omega_L$ rather than $4\Omega_L$. This is because the quadrupole moment must be

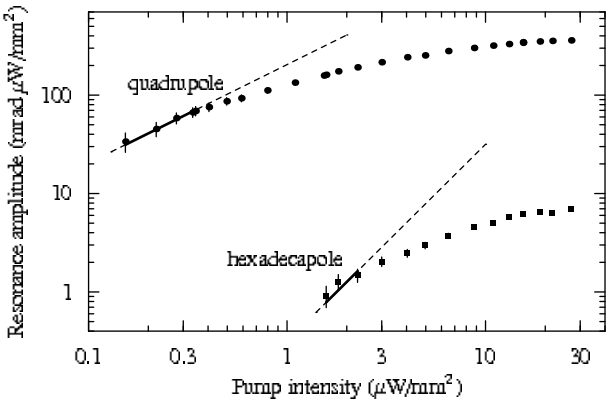

FIG. 6: The amplitude of the quadrupole and hexadecapole signals vs. pump-beam intensity for ^{87}Rb. The quadrupole signal grows linearly with pump-light intensity at low intensities, and then levels off due to saturation. Under these experimental conditions the hexadecapole signal was not large enough to be observed at intensities much below saturation. The two dashed lines show linear and quadratic slopes in pump intensity. The solid portions show the regions in which the experimental points obey linear and quadratic dependences, respectively. The intensity of the probe, tuned to the center of the $F = 2 \rightarrow F''$ transition group, was 1.6 μW/mm^2 and the pump-beam central frequency was tuned to the low-frequency wing of the $F = 2 \rightarrow F' = 1$ transition group.

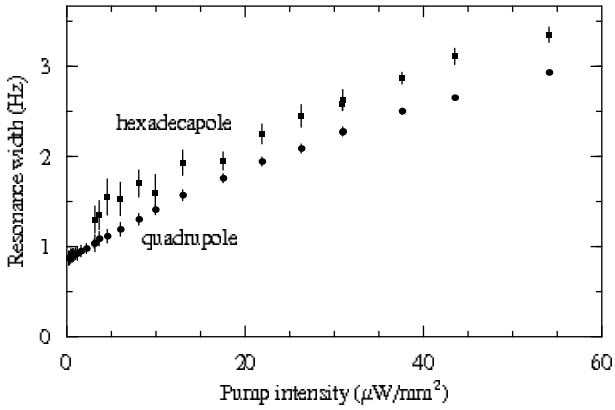

FIG. 7: The widths of quadrupole and hexadecapole resonances as a function of pump-beam intensity. The intensity of the probe is 1.6 μW/mm^2. Both beams were tuned the the same transitions as for the amplitude pump-intensity dependences (Fig. 6).

present in order to pump the hexadecapole moment, but the transverse quadrupole moment is averaged out when $\Omega_{mod} = 4\Omega_L$, as discussed in Section II, but will be not averaged out at $\Omega_{mod} = 2\Omega_L$. The signal due to the hexadecapole moment could then be separated from the quadrupole signal, in a two-beam arrangement, by detecting the signal at $4\Omega_L$ in an unmodulated probe. A detailed discussion of this point will be given elsewhere [18].

The widths of the quadrupole and hexadecapole FM NMOR resonances are plotted vs. pump intensity in Fig. 7. The experimental conditions are similar to those used for the measurement of the amplitude dependences. The low intensity of the probe (1.6 μW/mm^2) ensures that the power broadening of the signal due to the probe beam is small [33]. The widths of the resonances doubly extrapolated to zero pump- and probe-light intensity are $\delta\Omega^{(2)}_{mod} = 2\pi \times 0.85(5)$ Hz for the quadrupole moment and $\delta\Omega^{(4)}_{mod} = 2\pi \times 1.2(1)$ Hz for the hexadecapole moment, respectively. Since these widths are proportional to the relaxation rate of the respective multipoles, this implies that the quadrupole moment decays more slowly than the hexadecapole moment. The experimental ratio between the widths of the quadrupole and hexadecapole resonances doubly extrapolated to zero intensities of pump and probe beams is 0.7(1). This is in approximate agreement with the theoretical prediction of the electron randomization model [26] expected to be the main mechanism of relaxation, which gives the ratio as 9/16 [34]. Other mechanisms of relaxation [27] that are the same for both multipoles may contribute to the deviation between the experimental and theoretical ratio.

The quadrupole and hexadecapole spectra measured as a function of the pump-light central frequency are shown in Fig. 8. The probe laser was locked to the center of the $F = 2 \rightarrow F''$ transition group while the pump-beam central frequency was scanned over a range covering all hyperfine components of the D1 line. The signal in Fig. 8(a) related to the quadrupole moment was recorded with the modulation frequency fixed at 194 Hz, which was the frequency that produced the maximal rotation in the quadrature component of the signal. For the much smaller hexadecapole signal, we subtracted from the spectrum recorded at 388 Hz (the frequency producing the maximum quadrature hexadecapole signal) the spectrum measured for a modulation frequency detuned a few resonance widths away. This is done to remove the effect of the off-resonant background rotation on the recorded signal. The signal related only to the hexadecapole moment is shown in Fig. 8(b).

Because the $F = 2$ ground state can support both the quadrupole and hexadecapole moments, we would expect that signals due to both these moments would be observed for the pump beam tuned to the $F = 2 \rightarrow F'$ transition group, as Fig. 8 shows. However, the fact that signals related to both PMs are also observed for pump light tuned to the $F = 1 \rightarrow F'$ transition group is less intuitive. The polarization of the $F = 1$ ground state cannot be detected with the probe light tuned to $F = 2 \rightarrow F''$ which is only sensitive to the polarization of the $F = 2$ state. Furthermore, polarization cannot be transferred between the ground states via spin exchange because the two ground states experience rapid Larmor precession in opposite directions. Thus, the multipoles in the $F = 2$ state can only be generated indirectly in the following process. The pump beam tuned to the $F = 1 \rightarrow F'$

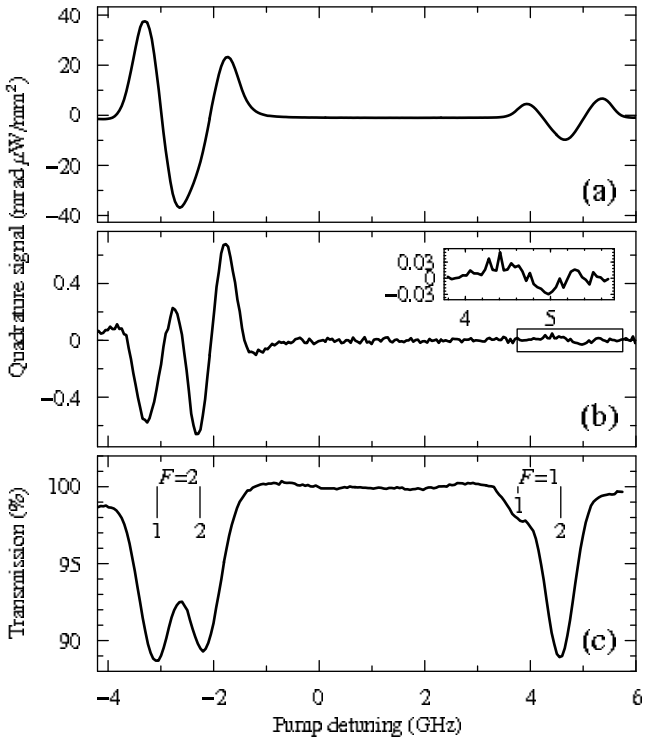

FIG. 8: The ^{87}Rb FM NMOR spectra as a function of the pump-light central frequency for the quadrupole (a) and hexadecapole (b) resonances along with the transmission spectrum (c). Note the different spectral dependences of the multipoles. The signal components observed at the $F = 1 \rightarrow F'$ transition result from the coherence transfer from the excited state F' to the $F = 2$ ground state via spontaneous emission (The inset shows the magnification of the signal related to the transfer of the $\Delta m = 4$ coherences). The vertical lines in plot (c) show the relative transition strengths of the $F \rightarrow F'$ hyperfine transitions, where the number below each line indicates the value of F'. The probe laser was tuned to the center of the $F = 2 \rightarrow F''$ transition group and its intensity was set to be 3.2 μW/mm^2. The pump intensity was 59 μW/mm^2. The absorption spectrum (c) was recorded at low light intensity (2.6 μW/mm^2).

transition group creates multipoles in the excited states. The $F' = 2$ state can support both the quadrupole and hexadecapole moments. The excited-state multipoles are then transferred to the $F = 2$ ground state via spontaneous emission. Such PM transfer has been observed previously for the case of the quadrupole moment [8, 28]. However, this is the first observation of the transfer of higher-order coherences.

B. Signature of the PMs

The amplitudes of the quadrupole and hexadecapole FM NMOR signals are plotted as a function of probe-light intensity in Fig. 9. The pump and probe beams have the same tuning and modulation frequencies as in

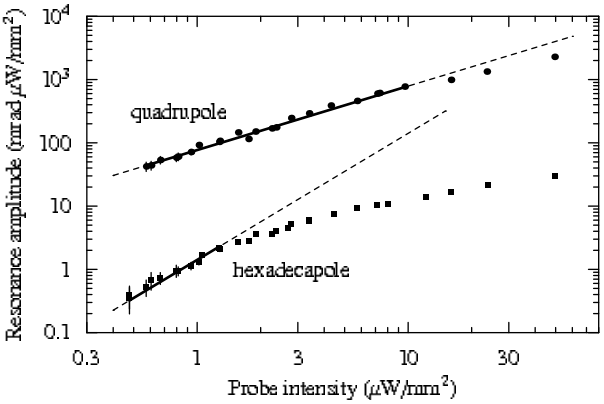

FIG. 9: The amplitudes of the quadrupole and hexadecapole signals vs. probe-light intensity at high pump-light intensity (70 μW/mm^2). The solid lines indicate the region in which the quadrupole has approximately linear and the hexadecapole approximately quadratic dependence on probe-beam intensity. The signals were recorded with the central frequency of the pump laser tuned to the low-frequency wing of the $F = 2 \rightarrow F' = 1$ transition and the probe beam tuned to the center of the $F = 2 \rightarrow F''$ transition group of ^{87}Rb.

the previous cases. The pump-beam intensity is high ($I_{pump} = 70$ μW/mm^2), enabling observation of the hexadecapole moment at relatively low probe-beam intensities.

For low probe intensity the amplitudes of the signals corresponding to both PMs asymptotically obey theoretical predictions: the quadrupole signal scales linearly and the hexadecapole quadratically with the probe-light intensity, the same as the pump-intensity dependence (see Fig. 6 for comparison). This is expected, as the same number of light-atom interactions is needed for creation and for detection of a given atomic PM. For both the quadrupole and hexadecapole signals, the products of the pump and probe intensity dependences are consistent with the intensity dependences previously observed in single-beam FM NMOR [7].

The widths of the quadrupole and hexadecapole resonances as a function of probe-beam intensity are shown in Fig. 10. To reduce the influence of pump-saturation effects on the measured signals the pump-light intensity was chosen to be relatively low (8 μW/mm^2). However, this pump-light intensity is still too high to allow for a reliable extrapolation to extract the intrinsic resonance widths.

With increasing probe-light intensity both resonances exhibit power broadening. The observed broadening is stronger than the broadening of the resonances measured as a function of pump-beam intensity (for comparison see Fig. 7) which is partly a result of the fact that the pump beam is modulated and so only periodically causes broadening and partly is due to different transition dipole moments of the D1 and D2 lines.

The measured spectral dependences of the quadrupole and hexadecapole resonances as a function of probe-beam

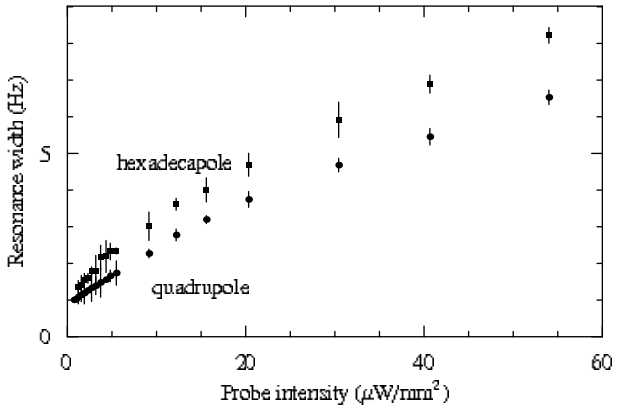

FIG. 10: The widths of the FM NMOR signals vs. probe-light intensity. The pump beam was tuned to the low-frequency wing of the $F = 2 \rightarrow F' = 1$ transition and the probe light was tuned near the center of the $F = 2 \rightarrow F''$ transition group of ^{87}Rb. The pump intensity was set to 8 μW/mm^2.

frequency are shown in Fig. 11. The probe frequency was scanned over all hyperfine components of the D2 line. The quadrupole signal is shown in Fig. 11(a), and the difference hexadecapole signal obtained in the same way as for the data presented in Fig. 8 is shown in Fig. 11(b). It is seen that the spectral dependences of the two signals are significantly different. They also differ from the spectra recorded vs. pump-beam central frequency (see Fig. 8 for comparison). The difference in frequency dependences for the pump and the probe beams illustrates the potential offered by the separated beam technique for optimization of the signal associated with a given PM.

Strong quadrupole and hexadecapole signals were observed when the probe light was tuned to the $F = 2 \rightarrow F''$ transition group. These PMs were produced directly by the pump light tuned to the low-frequency wing of the $F = 2 \rightarrow F' = 1$ transition. There was also very weak quadrupole signal measured when tuned to the $F = 1 \rightarrow F''$ transition group, which could only be produced by spontaneous decay of polarization from the upper state. We have verified with a calculation that the branching ratios are such that the generation of the quadrupole moment in the $F = 1$ ground state is strongly suppressed in this case. As expected, hexadecapole signal is not observed when probing the $F = 1$ ground state, which does not support the hexadecapole moment.

C. Creation and detection of hexacontatetrapole moment

The discussion in this subsection concerns data taken with ^{85}Rb, the $F = 3$ ground state of which can support the PM of rank $\kappa = 6$. Due to the fact that the averaged hexacontatetrapole moment has 6-fold symmetry (see Fig. 2(c)) the FM NMOR signals related to this multipole are observed at $\Omega_{mod} = 6\Omega_L$.

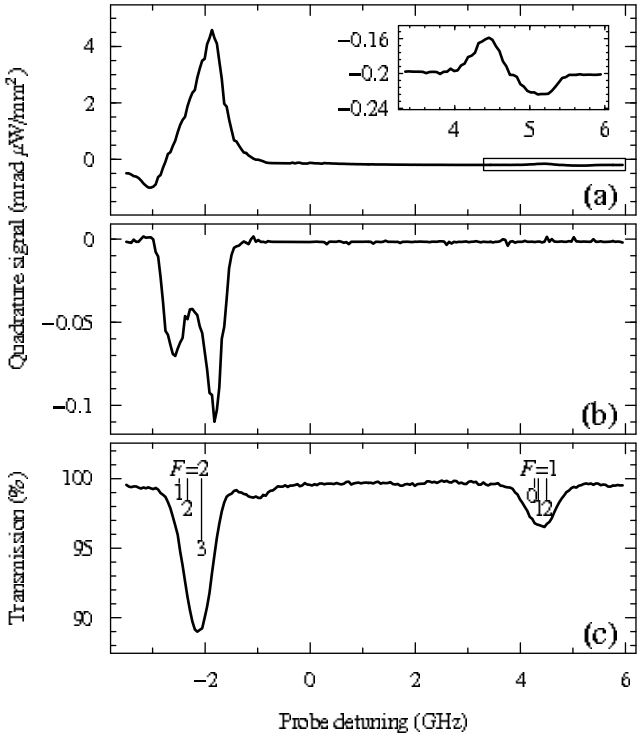

FIG. 11: Quadrupole (a) and hexadecapole (b) signal as a function of probe-beam frequency; (c) reference absorption spectrum of ^{87}Rb . The inset shows the magnification of the quadrupole signal related to the transfer of the coherences $\Delta m = 2$ from the excited $F' = 1$ or $F' = 2$ state to the ground state $F = 2$. In order to avoid saturation effects due to the pump light, the pump-beam intensity was relatively low (3.2 μW/mm^2). This entails the use of a high probe-beam intensity (57 μW/mm^2). The pump-beam central frequency was tuned to the low-frequency wing of the $F = 2 \rightarrow F' = 1$ transition.

The quadrupole, hexadecapole, and hexacontatetrapole signal amplitudes are plotted as a function of pump- and probe-beam intensities in Figs. 12 and 13, respectively. The pump-intensity dependence of the FM NMOR resonance related to the hexacontatetrapole moment is stronger than those of the quadrupole and hexadecapole resonances and is consistent with the expected I^3_{pump} dependence at low intensity. (Three photons are needed for the creation or detection of the hexacontatetrapole moment). The amplitudes of the quadrupole, hexadecapole and hexacontatetrapole resonances show, respectively, linear, quadratic, and cubic dependence on I_{probe} (Fig. 13).

The resonance-width dependences for the three multipoles are shown in Figs. 14 and 15. Although all resonances recorded as a function of pump-beam intensity (Fig. 14) broaden with the light intensity, the difference in the broadening is significant only in the first part of the measured dependences. The difference is due to the different number of photons needed to create the various multipoles. However, for higher pump-light intensities

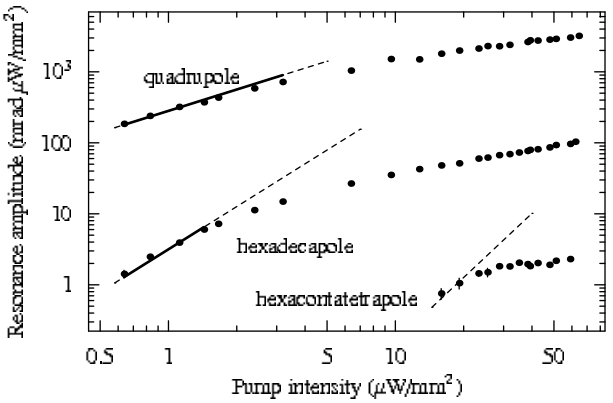

FIG. 12: The amplitudes of the FM NMOR resonances related to the quadrupole, hexadecapole and hexacontatetrapole moments in ^{85}Rb vs. pump-beam intensity. The dashed lines show linear, quadratic and cubic slopes while their solid parts indicate the region in which recorded dependences obey theoretical predictions. Under these experimental conditions (I_{probe} = 36 μW/mm^2) the measured amplitude dependence of the hexacontatetrapole signal is weaker than predicted cubic relation which is a result of saturation. The pump beam central frequency was tuned to the center of the $F = 3 \rightarrow F'$ transition group while the probe beam was tuned to the high-frequency wing of the $F = 3 \rightarrow F''$ transition group of ^{85}Rb.

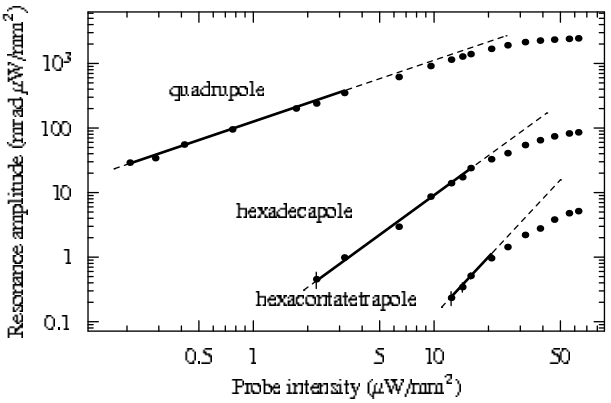

FIG. 13: The amplitudes of the FM NMOR signals related to the quadrupole, hexadecapole and hexacontatetrapole moments in ^{85}Rb as a function of probe-light intensity. The dashed and solid lines have the same meaning as in Fig. 12. The tuning of the pump beam was the same as in the previous case and its intensity was 52 μW/mm^2. The probe beam tuning was slightly different than in previous case and it was locked to the center of the $F = 3 \rightarrow F''$ transition group of ^{85}Rb. This difference in tuning of the probe-beam is a reason why the amplitudes of the FM NMOR signals presented in this plot are smaller than those in Fig. 12.

the saturation behavior starts to play an important role and all resonances exhibit similar broadening with the pump-light intensity i.e. slopes of the width dependences related to a given multipole are almost the same.

The width dependences of the FM NMOR signals on pump-beam intensity also show a very interesting feature. For a range of pump intensities the width of the hexadecapole resonance is broader than that of the hexaconatetrapole resonance. A more detailed analysis revealed that the ratio between these widths changes with the tuning of the pump and probe lasers. For instance, for the probe beam tuned toward higher frequencies the hexadecapole resonance is broader than the hexacontatetrapole resonance. The different tuning of the probe beam is the reason why similar behavior was not observed when signals were recorded as a function of probe-light intensity (Fig. 15).

In Fig. 16 the hexacontatetrapole signal, obtained using the method described in Section IV A, is shown as a function of pump-light central frequency. The probe light was tuned to the high-frequency wing of the $F = 3 \rightarrow F''$ transition group while the pump beam was scanned over all ^{85}Rb hyperfine components of the D1 line. Under these experimental conditions, a strong hexacontatetrapole signal was measured at the $F = 3 \rightarrow F'$ and $F = 2 \rightarrow F'$ transition group. The signal recorded at the $F = 2 \rightarrow F'$ transition group is a result of the hexacontatetrapole-moment transfer from the $F' = 3$ excited state to the $F = 3$ ground state via spontaneous emission, analogously to the situation described

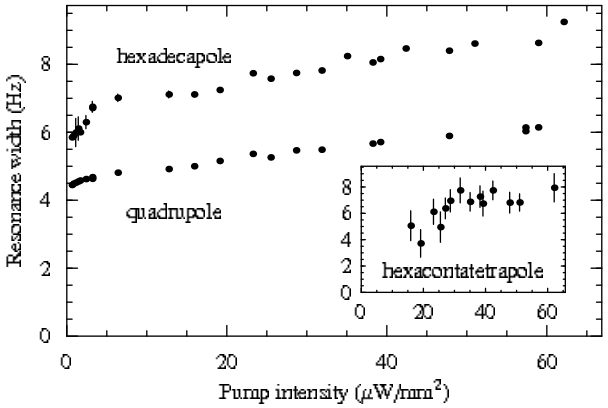

FIG. 14: The widths of the ^{85}Rb quadrupole, hexadecapole, and hexacontatetrapole (inset) FM NMOR resonances vs. pump-light intensity. The central frequency of the pump beam was tuned near the center of the $F = 3 \rightarrow F'$ transition group. The probe beam was tuned to the high-frequency wing of the $F = 3 \rightarrow F''$ transition group and its intensity was 36 μW/mm^2.

in Section IV A. The comparable amplitudes of the two spectral contributions show that the coherence-transfer mechanism could be very efficient. The amplitude of the hexacontatetrapole signal recorded at the $F = 2 \rightarrow F'$ transition group is comparable with the signal recorded at the $F = 3 \rightarrow F'$ transition group which directly supports creation of this type of the coherences in the ground state. This opens potential applications of this mechanism in the transfer of the Zeeman coherences between different atomic states.

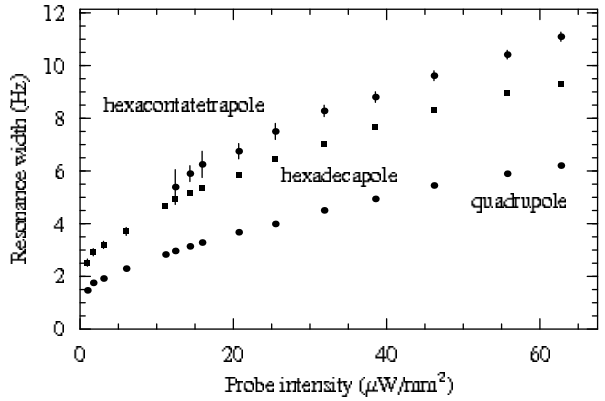

FIG. 15: The widths of the FM NMOR signals related to the quadrupole, hexadecapole and hexacontatetrapole moments vs. probe-light intensity. The pump beam central frequency was tuned to the center of the $F = 3 \rightarrow F'$ transition group and its intensity was 52 μW/mm^2. The probe beam was tuned to the center of the $F = 3 \rightarrow F''$ transition group.

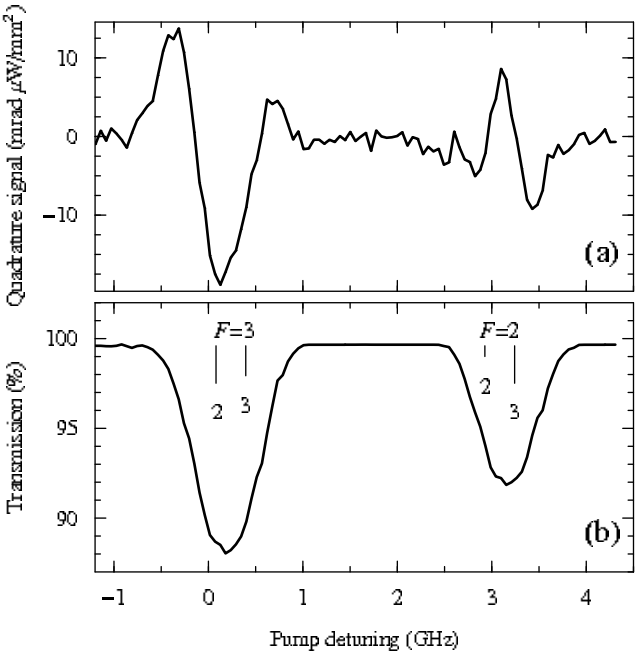

FIG. 16: Hexacontatetrapole signal (a) and the reference absorption spectrum taken with low light intensity (2.5 μW/mm^2) (b) vs. pump-beam central frequency recorded with ^{85}Rb. The strong hexacontatetrapole signal is measured at the $F = 3 \rightarrow F'$ transition group which supports generation of this multipole in the ground state. The hexacontatetrapole signal is also observed for the pump-light tuned to the $F = 2 \rightarrow F'$ transition group which does not support creation of the quadrupole in the ground state. This signal is due to the transfer of the coherences from the excited state $F' = 3$ to the ground state $F = 3$ via spontaneous emission. The probe laser was tuned to the center of the $F = 3 \rightarrow F''$ transition group, while pump-light central frequency was scanned over all hyperfine components of ^{85}Rb D1 transition. For the measurements of the signal related to the hexacontatetrapole moment the pump-beam intensity was 64 μW/mm^2 and probe-beam intensity was 65 μW/mm^2.

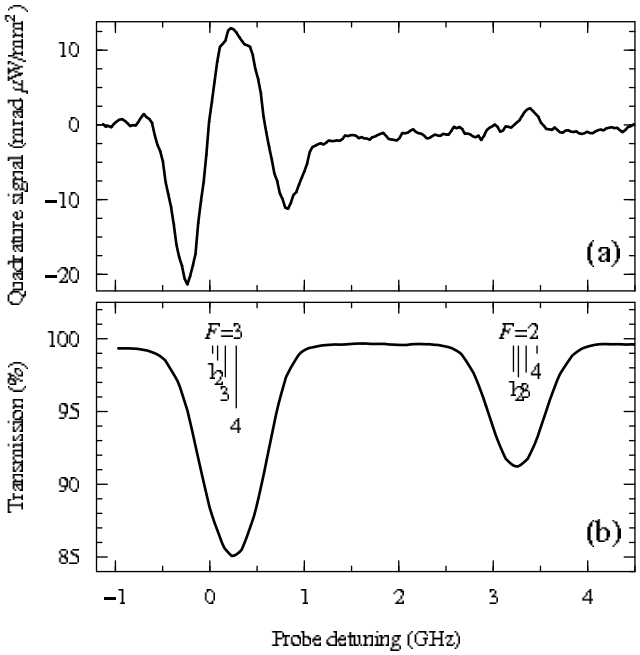

FIG. 17: The signal related to the hexacontatetrapole moment (a) and the reference spectrum taken for low light intensity (b) vs. probe-light frequency. The central frequency of the pump beam was tuned to the center of the $F = 3 \rightarrow F'$ transition group while the probe-beam frequency was scanned over all hyperfine components of the ^{85}Rb D2 line. The pump- and probe-beam intensities were chosen to be the same as in Fig. 16.

In Fig. 17 the hexacontatetrapole signal is shown as a function of probe-beam frequency. The spectrum was recorded for the pump-light central frequency tuned to the high-frequency wing of the $F = 3 \rightarrow F'$ transition group. The probe beam was scanned over all hyperfine components of the ^{85}Rb D2 line. The pump- and probe-beam intensities were the same as for the previous case. The hexacontatetrapole signal is seen only for the probe beam tuned to the $F = 3 \rightarrow F''$ transition group, as expected.

V. CONCLUSION

We have studied the processes of creation and detection of atomic PMs using the FM NMOR method in a two-beam pump-probe arrangement. The separated pump and probe beams allow a detailed analysis of these processes as a function of a number of light-beam parameters such as intensity, detuning from resonance, and modulation frequency. The influence of these parameters on the amplitudes and widths of the FM NMOR resonances has been studied. Working with two rubidium isotopes, all even-rank PMs supported by the atomic energy level structure have been detected. It has been shown that signals due to the quadrupole, hexadecapole, and hexacontatetrapole moments depend differently on the

frequency and intensity of the pump and probe beams. This may be used for a more complete optimization of the system than it is possible in a one-beam arrangement. In particular, a given PM's contribution can be zeroed or maximized, which may be significant for many applications, especially magnetometry in the Earth-field range. We have also observed for the first time the transfer of high-rank moments from the excited to the ground state via spontaneous emission which may be useful for creating high-order ground state coherences with minimal light-power broadening of the FM NMOR resonances.

Acknowledgments

The authors acknowledge fruitful discussion with Jerzy Zachorowski and Marcis Auzinsh. S.P. and W.G. would like to thank their colleagues from UC Berkeley for their hospitality. This work has been supported by National Science Foundation (grant: 2003-06 INT-0338426), NATO (grant: PST.CLG980362) and by the ONR MURI program.

[1] E. B. Alexandrov, M. Auzinsh, D. Budker, D. F. Kimball, S. M. Rochester, and V. V. Yashchuk, J. Opt. Soc. Am. B **22**, 7 (2005).
[2] D. Budker, W. Gawlik, K. F. Kimball, S. M. Rochester, V. V. Yashchuk, and A. Weis, Rev. Mod. Phys. **74**, 1153 (2002).
[3] J. Vanier, Appl. Phys. B, **81**, 421 (2005).
[4] D. Budker, V. Yashchuk, and M. Zolotorev, Phys. Rev. Lett. **81**, 5788 (1998).
[5] D. Budker, L. Hollberg, D. F. Kimball, J. Kitching, S. Pustelny, and V. V. Yashchuk, Phys. Rev. A **71**, 012903 (2005).
[6] W. Bell and A. Bloom, Phys. Rev. Lett. **6**, 280 (1961).
[7] V. V. Yashchuk, D. Budker, W. Gawlik, D. F. Kimball, Y. P. Malakyan, and S. M. Rochester, Phys. Rev. Lett. **90**, 253001 (2003).
[8] E. B. Alexandrov, M. P. Chaika, and G. I. Khvostenko, Interference of Atomic States (Springer, New York, 1993).
[9] B. Łobodziński and W. Gawlik, Phys. Rev A. **54**, 2238 (1996).
[10] D. Suter, T. Marty, and H. Klepel, J. Opt. Soc. Am. B **11**, 531 (1993).
[11] A. B. Matsko, I. Novikova, G. R. Welsh, and M. S. Zubairy, Opt. Lett. **28**, 96 (2004).
[12] Q. A. Turchette, C. J. Hood, W. Lange, H. Mabuchi, and H. J. Kimble, Phys. Rev. Lett. **75**, 4710 (1995).
[13] S. E. Harris, Phys. Today **50**, 36 (1997).
[14] E. Arimondo, Prog. Opt. **25**, 257 (1996).
[15] E. B. Alexandrov, M. V. Balabas, and J. L. Rasson, Laser Physics **6**, 244 (1997).
[16] A. I. Okunevich, Opt. Spectrosk. **91**, 193 (2001).
[17] M. Stahler, S. Knappe, C. Affolderbach, W. Kemp, and R. Wynands, Europhys. Lett. **53**, 323 (2001).
[18] W. Gawlik, M. Auzinsh, S. Pustelny, S. M. Rochester, D. F. Kimball, and D. Budker – to be published.
[19] S. M. Rochester and D. Budker, Am. Journ. Phys. **69**, 450 (2001).
[20] D. Budker, D. F. Kimball, V. V. Yashchuk, and M. Zolotorev, Phys. Rev. A **65**, 055403 (2002).
[21] Y. P. Malakyan, S. M. Rochester, D. Budker, D. F. Kimball, and V. V. Yashchuk, Phys. Rev. A **69**, 013817 (2004).
[22] D. Budker, V. V. Yashchuk, and M. Zolotorev, in Trapped Charged Particles and Fundamental Physics, edited by D. H. E. Dublin and D. Schneider (American Institute of Physics, New York, 1999), pp. 177-182.
[23] G. Wąsik, W. Gawlik, J. Zachorowski, and W. Zawadzki, Appl. Phys. B **75**, 613 (2002).
[24] V. V. Yashchuk, D. Budker, and J. R. Davis, Rev. Sci. Inst. **71**, 341 (2000).
[25] D. Budker, D. F. Kimball, S. M. Rochester, and V. V. Yashchuk, Phys. Rev. Lett. **85**, 2088 (2000).
[26] W. Happer, Rev. Mod. Phys. **44**, 169 (1972).
[27] M. T. Graf, D. F. Kimball, S. M. Rochester, K. Kerner, C. Wong, D. Budker, E. B. Alexandrov, M. V. Balabas, and V. V. Yashchuk, Phys. Rev. A **72**, 023401 (2005).
[28] M. Auzinsh and R. S. Ferber, Opt. Spectrosc. **66**, 158 (1989).
[29] D. Budker, D. F. Kimball, S. M. Rochester, and V. V. Yashchuk, Phys. Rev. A **65**, 033401 (2002).
[30] Magneto-optical rotation in pump-probe arrangement without frequency modulation has been studied previously (see Section 8c in Ref. [2] and references therein).
[31] At high light power, odd rank PMs can be generated with a magnetic field present [25].
[32] The rotation of the polarization plane due to the Bennett-structure effect (see, for example, Ref. [29]) is negligible in our experiment.
[33] While the width dependences of both PMs shown in Fig. 7 look similar, the detailed mechanisms responsible for the two broadenings are dierent. This is due to the fact, that higher-order multipoles are created from the lower-rank PMs by interaction with additional photons. In consequence, just as more photons are needed to create higher-rank PMs, more photons contribute also to their saturation. Although the exact functional dependences of the widths of the FM NMOR resonances vs. light power is unknown we approximate them with linear dependences in low-light limit.
[34] In Ref. [7], the expected ratio of the relaxation was erroneously quoted as 3/8 (instead of 9/16). This change of the numerical value does not affect the qualitative conclusions reached in that paper. The experimental results in Ref. [7] corresponds to $\delta\Omega^{(2)}_{mod}/\delta\Omega^{(4)}_{mod} = 0.47(4)$.